

stress and strain data points, mathematical equations were fitted using these data points for use in the static analysis model of CFFT beams, to facilitate computer programming. The FRP material is assumed to be linear elastic in tension and in compression.

Cyclic Loading Analysis

The static model described in the previous section was extended to model CFFT beams under reversed cyclic bending, by introducing time dependent changes in the stress-strain relationships of the materials. The main goal of the analysis is to trace the moment-curvature response of a section at any given time or at the equivalent number of cycles, if the frequency of the applied load is kept constant throughout the loading history. In order to analyze a CFFT beam under cyclic bending, constitutive models for creep and fatigue of the different materials need to be incorporated.

When a CFFT member is subjected to a reversed bending moment, during the first half of each cycle the moment will be in a certain direction, causing tension on one side and compression on the other. In the second half of the cycle, the direction of the moment is reversed and so are the tension and compression sides, as shown in **Figure 6**. Experimental results and static models have shown that the position of the neutral axis remains quite stable after cracking of the concrete and up to about 70% of the ultimate bending moment. Therefore, it could be assumed that the location of the neutral axis remains unchanged during each half cycle of loading. As such, layers located between the extreme top (or bottom) fibers of the section and a distance equals to the neutral axis depth from the top (or bottom) will be subjected to compression in one half of the cycle and tension in the other half of the cycle, as shown in **Figure 6**. On the other hand, layers within the middle of the section will always be subjected to tension, but at a lower level.

The contribution of concrete in tension is generally neglected when modeling the cyclic behavior of reinforced concrete members. Additionally, the reversed cyclic bending results in full-depth cracks, as mentioned previously. It is therefore a reasonable assumption to neglect the contribution of concrete in tension. The stress in concrete layers during cycling is assumed to follow the same function as the loading and could therefore be represented by a series of half sine waves with the minimum stress equals to zero, as shown in **Figure 7**, where duration of the loading in compression is approximated as half the time of each cycle.

Fatigue and creep models for concrete under compression -- Holmen (1982)¹⁰ suggested that the total strain for concrete subjected to cyclic loading in compression can be expressed as the sum of two components, as follows:

$$\varepsilon_{tot} = \varepsilon_e + \varepsilon_{cr} \quad (1)$$

where, the first term ε_e is related to the endurance of the concrete specimen, and the second term ε_{cr} , is a function of the loading time, and is essentially a creep strain.

It was observed from tests¹⁰ that three distinct strain development phases could be observed. A rapid increase phase until about 10% of the fatigue life, followed by a uniform increase phase until about 80% of the fatigue life, and finally another rapid increase phase until failure. Holmen (1982)¹⁰ suggested the following equation to predict the total strain in the first two phases.

$$\varepsilon_e = \varepsilon_o \left| 1 + \frac{3.18}{S_{max}} (1.183 - S_{max}) \left(\frac{N}{N_f} \right)^{0.5} \right| \quad \text{for } 0 < \frac{N}{N_f} \leq 0.1 \quad (2)$$

$$\varepsilon_e = \frac{1.11\varepsilon_o}{S_{max}} \left| 1 + 0.677 \frac{N}{N_f} \right| \quad \text{for } 0.1 < \frac{N}{N_f} \leq 0.8 \quad (3)$$

$$\varepsilon_{cr} = 0.413 \times 10^{-3} S_c^{1.184} \ln(t+1) \quad \text{for both phases} \quad (4)$$

where ε_o is the maximum total strain in the first load cycle, N is the number of cycles, and N_f is the total number of cycles to failure calculated by

$$\log_{10} N_f = 1.978 \left(S_{max}^{-3.033} \right) (-\log_{10} L_p)^{-0.596} \quad (5)$$

where L_p is $1-p$ or the complimentary probability, and p is the probability of failure usually taken as 0.95. S_{max} is the ratio of the applied maximum stress level σ_{max} to the unconfined concrete strength f'_c . S_c is the characteristic stress level or sum of the mean stress level and the root mean square value, calculated as follows:

$$S_c = S_m + RMS \quad (6)$$

where the mean stress level $S_m = (S_{max}+S_{min})/2$, and S_{min} is the stress ratio for the minimum applied stress level, equals to the ratio of σ_{min} to the unconfined concrete strength f'_c . The root mean square value (RMS) is defined as

$$RMS = \sqrt{\frac{1}{T_o} \int_0^{T_o} f^2(t) dt} \tag{7}$$

where $f^2(t)$ is the stress at any given time t , and T_o is the entire duration of the cyclic loading. The RMS value of a sinusoidal loading with amplitude of $(S_{max} - S_{min})/2$ is given by

$$RMS = \frac{(S_{max} - S_{min})}{2\sqrt{2}} \tag{8}$$

Hence:
$$S_c = \left(\frac{S_{max} + S_{min}}{2} \right) + \left(\frac{S_{max} - S_{min}}{2\sqrt{2}} \right) \tag{9}$$

This model has been widely accepted and incorporated in the model by Deskovic (1993)⁷ for hybrid concrete/FRP beams and by El-Tawil et al. (2001)¹³ to model reinforced concrete beams strengthened with FRP sheets. Although this model has been developed based on experimental results of unconfined concrete it was successfully used by Ahmad (2004)² to model CFFT beams subjected to a cyclic loading (none reversed bending) by replacing the unconfined concrete strength f'_c with the confined concrete strength f'_{cc} .

Fatigue, creep and stiffness degradation models for GFRP – Helmi et al. (2007)⁶ conducted an extensive experimental fatigue study on coupons cut from similar tubes to the ones used in the CFFT full scale tests. The test data was used to calibrate the empirical model by Epaarachchi and Clausen (2003)¹⁴, which was developed to curve-fit fatigue test data. The method uses a single nonlinear function to represent the entire range of maximum-to-ultimate stress ratio σ_{max}/σ_u ratios. The method also could predict the fatigue life for different frequencies f and minimum-to-maximum stress ratios R , beyond the range used to fit the curves. The following equations are used:

$$\frac{D}{\alpha} = (N^\beta - 1) \tag{10}$$

where;
$$D = \left(\frac{\sigma_u}{\sigma_{max}} - 1 \right) \left(\frac{\sigma_u}{\sigma_{max}} \right)^{0.6 - \psi |\sin \theta|} \left[\frac{1}{(1 - \psi)^{1.6 - \psi |\sin \theta|}} \right] f^\beta \tag{11}$$

$$\psi = R \quad -\infty < R < 1 \text{ (tension - tension and tension - compression)} \tag{12}$$

$$\psi = 1/R \quad 1 < R < \infty \text{ (compression - compression)}$$

α and β are curve fitting parameters, which were calibrated using the tests conducted by Helmi et al. (2007)⁶; f is the frequency of the applied load; θ is the smallest angle of fibers between the loading and fiber directions, and N is the number of cycles.

It is worth noting that this fatigue life model, which is basically for GFRP coupons, was extrapolated, as a simplified approximation, to directly represent fatigue life of a complete CFFT system⁶. This was done in lieu of the rigorous analysis presented in this paper for the complete CFFT system. It was recognized, however, that this approximation does not account for the effect of fatigue on concrete, nor does it account for the redistribution in stresses that occurs in full scale specimens due to the loss of stiffness in both the concrete and the FRP tube during cycling.

Findley (1960)⁹ proposed the following empirical power law to describe total strain at time t for polymers and FRP laminates subjected to sustained loads;

$$\epsilon_{cr} = \epsilon_o (1 + mt^{nc}) \tag{13}$$

where ϵ_o represents instantaneous strain at time $t = 0$, m and nc are material dependant parameters obtained from experimental data, and t is the duration of sustained load, usually in hours. The net creep strain ϵ_{cm} could be calculated as

$$\epsilon_{cm} = \epsilon_o mt^{nc} \tag{14}$$

An FRP coupon subjected to repeated loading will undergo an increase in strain. This increase can be divided into two components, the first component is due to the reduction in the elastic modulus (i.e. stiffness degradation) and the second component is due to creep, as shown in Figure 8. The total strain could then be calculated as follows⁷;

$$\varepsilon_{tot} = \frac{1}{\phi(\sigma_{max}, N)} \varepsilon_o + \varepsilon_{crm} \quad (15)$$

where ε_o is the initial undamaged strain. Since the applied stress is variable, the characteristic stress for the FRP, S_{cf} , is used in a similar manner to the equations suggested by Holmen (1982)¹⁰ for concrete, to calculate the creep in the FRP tube. Therefore, Equation 15 becomes

$$\varepsilon_{tot} = \varepsilon_o \left(\frac{1}{\phi(\sigma_{max}, N)} + S_{cf} m t^{nc} \right) \quad (16)$$

Fibers of the tube located at equal distances from mid height of the sections in a CFFT beam subjected to reversed cyclic bending will alternate their maximum and minimum values of strains in each cycle, as shown in **Figure 6**. These elements will effectively have the same maximum and minimum strains, and since a linear relation is assumed for FRP, they will have the same maximum and minimum stresses. Consequently, they will suffer the same degradation in the elastic modulus and will have the same permanent creep deformation resulting from the cyclic loads. All elements at equal distance from the midheight of the sections must be considered simultaneously when solving for the time dependent deformations of FRP elements in a CFFT beam subjected to reversed cyclic bending as follows

$$\varepsilon_o^{\max} = \frac{\varepsilon_{tot}^{\max}}{\left(\frac{1}{\phi(\sigma_{max}, N)} \right) + S_{cf} m t^{nc}} \quad (17)$$

$$\varepsilon_{crm} = S_{cf} \varepsilon_o^{\max} (m t^{nc}) \quad (18)$$

$$\varepsilon_o^{\min} = \frac{\varepsilon_{tot}^{\min} - \varepsilon_{crm}}{\left(\frac{1}{\phi(\sigma_{max}, N)} \right)} \quad (19)$$

where;

$$S_{cf} = \frac{1+R}{2} + \frac{1-R}{2\sqrt{2}} \quad (20)$$

$$R = \frac{\sigma_{max}}{\sigma_{min}} \quad (21)$$

A creep test was conducted by the authors on 25 mm (1 in.) wide strip cut from the tubes used in this study to calibrate the parameters of Findley' model. The experimental results yielded a value of 0.0434 for m and a value of 0.143 for nc .

Ogin et al. (1985)⁸ developed an equation for calculating the stiffness degradation of $[0^\circ/90^\circ]$ laminates assuming linear relationship between the elastic modulus and crack density, and the total crack length, as the power function of the stored elastic energy, given by

$$-\frac{1}{E_0} \frac{dE}{dN} = A \left(\frac{\sigma_{max}^2}{E_0^2 \left(1 - \frac{E}{E_0} \right)} \right)^{ng} \quad (22)$$

where $\left[-\frac{1}{E_0} \frac{dE}{dN} \right]$ is the modulus reduction rate at a given value of E/E_0 , E_0 is the uncracked elastic modulus, E is the secant modulus of FRP at a given number of cycles N , and σ_{max} is the maximum applied stress. By integrating Equation 22, the following function is obtained for the stiffness degradation⁷

$$\frac{E}{E_0} = 1 - [(ng + 1)A]^{1/ng+1} \left[\frac{\sigma_{max}}{E_0} \right]^{2ng/ng+1} [N]^{1/ng+1} \quad (23)$$

Using coupon test data⁶ to calibrate the material constants A and ng in Equation 23 resulted in the following relations for the stiffness degradation expressions:

$$\phi(\sigma_{\max}, N) = \frac{E_{ftN}}{E_{ft0}} = 1 - 393 \left[\frac{\sigma_{\max}}{E_{ft0}} \right]^{1.608} \left[\frac{N}{N_f} \right]^{0.196} \quad (\text{Tension}) \quad (24)$$

$$\phi(\sigma_{\max}, N) = \frac{E_{fcN}}{E_{fc0}} = 1 - 1100 \left[\frac{\sigma_{\max}}{E_{fc0}} \right]^{1.67} \left[\frac{N}{N_f} \right]^{0.167} \quad (\text{Compression}) \quad (25)$$

where E_{ft0} is the initial modulus of elasticity for FRP in tension, E_{fc0} is the initial modulus of elasticity for FRP in compression, E_{ftN} is the modulus of elasticity for FRP in tension after N cycles, E_{fcN} is the modulus of elasticity for FRP in compression after N cycles, σ_{\max} is the maximum stress, and N_f is the number of cycles to failure.

As indicated earlier, in the case of reversed cyclic bending, some layers of the materials will be subjected to tension-tension fatigue while others will be subjected to tension-compression fatigue. It has been shown that specimens subjected to tension-compression fatigue suffer more damage per cycle than specimens subjected to tension-tension fatigue¹⁵.

Estimation of fatigue life of full scale CFFT beams -- The experimental results of the full-scale CFFT beams showed that the specimens fail in tension at the extreme fibers. Therefore, the fatigue life could be estimated by calculating the damage at the extreme top and bottom fibers. As explained earlier, at the beginning of cycling, the top and bottom fibers will alternate the maximum and minimum stresses and strains, producing certain $\sigma_{\max}/\sigma_{ult}$, and R values that will produce a certain fatigue life N_f . As the cyclic loading progresses, there will be a redistribution of the stresses along the section and the values of the stresses and strains at the extreme fibers will change and so will the $\sigma_{\max}/\sigma_{ult}$ and R values, and as a result, the value of the fatigue life N_f will change. If a linear accumulative damage model is assumed, and since the analysis is conducted at discrete time steps, the damage DMG at a certain calculation step k could be calculated as the ratio of the number of cycles at this step to the average number of cycles to failure N_f at the beginning and the end of this step as follows

$$DMG_k = \frac{N_k - N_{k-1}}{\left(\frac{N_{f(k)} + N_{f(k-1)}}{2} \right)} \quad (26)$$

and for the first calculation step the damage is calculated by

$$DMG_1 = \frac{1}{N_{f(1)}} \quad (27)$$

where DMG_k is the damage at time step k , N_k is the number of cycles at time step k , and $N_{f(k)}$ is the number of cycles to failure calculated at step k . The total damage DMG_{tot} at a time step k could be calculated as;

$$DMG_{tot} = \sum_{k=1}^k DMG_k \quad (28)$$

Failure will occur when DMG_{tot} is equal to unity.

Modeling Procedure

A FORTRAN program was developed for the reversed cyclic bending analysis of CFFT beams with the following steps:

1. Input of geometric and material properties of the section, number of layers n , number of sections along the span ns , stiffness degradation and creep properties (i.e. m , nc , A , ng , α , β), and frequency of applied load f .
2. Calculate the area of each layer.
3. Input the moment at the midspan section M_t , at which the values of deflection and strain profile are required.
4. Start with number of cycles $N=1$.
5. Calculate time t : $t=N/f$ for FRP layers, and $t=N/2f$ for concrete layers.
6. At each section j calculate the bending moment as $M_j = M_t \frac{j}{ns}$
7. Assume a bottom strain ϵ_b .
8. Assume a depth of the neutral axis C .
9. Calculate the total strains ϵ_{tot} in each layer from the linear strain profile.
10. Calculate an initial value for the stress σ_i at each layer from the undamaged static constitutive models.
11. Calculate the initial strain ϵ_o for each layer as follows;

For concrete: Calculate $S_{\max} = \frac{\sigma_i}{f'_{cc}}$, $S_{\min} = 0$, N_f , S_c , ε_{cr}^i , and ε_o^i . For FRP: $\sigma_{\max} = \sigma_i$ and $\sigma_{\min} = \sigma_{(n-i+1)}$,

calculate $R = \frac{\sigma_{\max}}{\sigma_{\min}}$, N_f , S_{cf} , $\phi(\sigma_{\max}, N)$, ε_o^{\max} , ε_{cr}^i , and ε_o^{\min} .

12. Calculate the stresses σ'_i at each layer from the undamaged static constitutive models based on the calculated initial strain ε_o . σ'_i is compared to σ_i , and if the difference is less than a specified tolerance, σ_i is changed to $(\sigma_i + \sigma'_i)/2$ and steps 11 and 12 are repeated until convergence is achieved. If $i = 1$ and $j = ns$, then $N_{f(k)}$ is N_f which was calculated in step 11 – iii.
13. Calculate the forces at each layer by multiplying the stress and the area.
14. Calculate the moment at each layer by multiplying the force by the distance from the neutral axis.
15. Check for force equilibrium. In this case the total force must be equal to zero under constant bending. If force equilibrium is not satisfied change the neutral axis depth and repeat steps 8 to 15 until convergence is achieved.
16. Calculate the total moment at the section and compare to M_j , if the difference is less than the specified tolerance change the value of the bottom strain ε_b and repeat steps 7 to 16 until convergence is achieved.
17. Calculate the curvature of the section $\psi = \varepsilon_b / (D_t - C)$
18. Repeat steps 6 to 17 for each section.
19. Integrate the moment curvature profile numerically along the span to calculate the deflection using the moment area method.
20. Calculate the total damage
21. If DMG_{tot} is less than one increase the number of cycles in step 4 and repeat steps 5 to 20, otherwise terminate the program.

The fixed point iteration method was used for stress convergence. However, iteration step was taken as $(\sigma_i + \sigma'_i)/2$. For force and moment equilibrium the secant method of iteration was used. The first two estimates were selected using the ranges obtained from static analysis as guidance.

Verification of the Model

Figure 9 shows the results of the fatigue life estimation of the full-scale CFFT specimens, compared to the experimental results. Error bars representing the scatter of the experimental fatigue results of GFRP coupons of the same tubes tested at the corresponding stress levels to the moments at which the CFFTs were tested have been superimposed on the data points of the CFFT specimens. Since some slip between the concrete core and the GFRP tube has been observed in the test specimens, upper and lower bound predictions have been established for fatigue life as shown in Figure 9. One is established assuming that the concrete is totally inactive (i.e. excessive slip has taken place to the extent that concrete discontinuity has occurred at the location of the full depth crack) and the entire load is carried by the tube. The other prediction is established assuming full composite action between the concrete core and the tube. It is apparent from the figure that the full composite action model overestimates fatigue life at high M_{\max}/M_{ult} values. This is attributed to the slip that occurred during testing, which is not accounted for in the model. On the other hand, ignoring the concrete core completely has under estimated fatigue life. The experimental results lay between the two predicted curves. It is safe to say, however, that in real life applications a more composite action would occur because of end restraints imposed by joints to other members, which would minimize slip, and hence, the full composite action assumption is more realistic. This is confirmed by that fact that it lead to the best prediction at the lowest M_{\max}/M_{ult} ratio of 0.35, as slip was minimal. at this moment.

The model predictions were also compared to the test results of specimens BFC1, BFP1U and BFC3 in terms of deflection and strain histories. Figures 3 and 5 show a comparison between the experimental and analytical results with regard to deflection and strains versus the number of cycles. The analysis for specimen BFC1 was carried out for the first 670,000 cycles of loading only, due to the change of the loading frequency that occurred afterwards. The analytical results show good agreement with the experimental results. The experimental results from specimen BFC1 show stiffer response than the analytical solution. This may be attributed to the fact that the maximum moment at the midspan section for this specimen was 50 kN.m and the cracking moment was about 18 kN.m. As such, a significant length of the member was uncracked and had higher stiffness than calculated by the model which ignores the contribution of concrete in tension. Additionally, since the maximum moment is low, the

effect of the tension stiffening relative to the over all behavior will be higher than for the other specimens, which had much higher mid span moments.

PARAMETRIC STUDY

A parametric study was conducted using the computer program developed, based on the procedures described earlier. Three different tube diameters were considered, namely, 256 mm (10 in.), 367 mm (14.4 in.), and 456 mm (18 in.). The same thickness and properties for all the tubes were assumed to be the same as the tubes used in the experimental study and discussed earlier, to achieve different FRP reinforcement ratios. Since the tube diameter-to-thickness ratio would affect the confinement effectiveness of the concrete, a stress-strain relation was constructed for each tube diameter using the model developed by Fam and Rizkalla (2001)¹². A group of curves were then fitted to this data for programming purposes. A static analysis was conducted for all tubes. For each tube diameter, two different maximum loading levels were considered in reversed bending, namely 25% and 50% of the ultimate bending moment calculated from the static analysis. These service load levels were chosen as they represent factors of safety of 2 and 4. For each load level, two loading frequencies were considered, namely 1 and 5 Hz. For each combination of tube diameter, maximum loading level and frequency, three loading cases were considered. The first case considers the effect of the time dependant properties of both the tube and concrete. The second case only considers the time dependant properties of the tube, and ignores those of concrete. The third case considers the time dependant properties of the concrete only, and ignores those of FRP. In total 36 analyses were conducted to study the effect of the different parameters on the behavior of CFFT members subjected to reversed cyclic bending, in terms of deflection, top and bottom strains, and neutral axis depth throughout the loading history. Only representative curves of these results are presented in this paper. The entire results of all the analyses can be found in Helmi (2006)⁴.

Effect of Time Dependant Properties of Materials

Figures 10 (a, b and c) presents sample curves of the history of strains, neutral axis depth, and deflection versus N/N_f , respectively, for the three different cases of time dependant properties for a maximum moment of 50% of the ultimate. It is apparent from these figures that both the concrete and FRP time dependant properties have some effect on the deflection behavior of CFFT members subjected to reverse cyclic bending. It is also apparent that the time dependant properties of the FRP tube have a more significant effect on the increase in the bottom strain. On the other hand, the time dependant properties of concrete have a more significant effect on the increase in the top strain. The depth of the neutral axis tends to increase when only considering the time dependant properties of concrete, and tends to decrease when only considering the time dependant properties of the tube.

Effect of Loading Frequency and Load Level

Figures 11(a, b and c) present sample curves of the relative bottom strain ($\epsilon_b/\epsilon_{bstatic}$), top strain ($\epsilon_t/\epsilon_{tstatic}$), and the relative deflection (δ/δ_{static}), plotted versus N/N_f , respectively, for the two maximum loading levels and the two loading frequencies. It is apparent from these curves that increasing the loading frequency decreases the deterioration in the response of CFFT members, in terms of the excessive deflections or strains. The same is true for the maximum loading level, at the same N/N_f ratios. However, this will be the opposite for the same number of cycles N .

Effect of Tube Diameter (i.e. FRP Reinforcement Ratio)

Figures 12(a, b and c) present sample curves of the relative bottom strain ($\epsilon_b/\epsilon_{bstatic}$), top strain ($\epsilon_t/\epsilon_{tstatic}$) and the relative deflection (δ/δ_{static}), plotted versus N/N_f , respectively, for the three tube diameters. It is apparent from these figures that the larger diameter members (i.e. with smaller FRP reinforcement ratio) will suffer slightly larger deterioration in their cyclic response than CFFT of smaller diameter (i.e. with larger FRP reinforcement ratio). Figure 13 shows the variation of number of cycles to failure N_f with FRP reinforcement ratio, which reflects the diameter-to-thickness ratio. The figure clearly shows that the diameter-to-thickness ratio has insignificant effect on fatigue life.

CONCLUSIONS AND RECOMMENDATIONS FOR FURTHER STUDIES

1. The analytical method presented in this paper predicts reasonably well fatigue life curves and time dependent responses of CFFT specimens subjected to reversed cyclic bending.
2. Excessive slip between the concrete core and FRP tube could reduce fatigue life. This reduction is further increased as the maximum applied moment is increased.
3. Both the concrete and FRP time dependant properties have a significant contribution to the long term behavior of CFFT members subjected to reverse cyclic bending.
4. Increasing loading frequency causes less deterioration (excessive deflection) in the response of CFFT members, whereas the opposite is true for the load level at which cyclic loading is applied.
5. The diameter-to-thickness ratio of the FRP tubes has insignificant effect on the fatigue life of the system. However, tubes with larger diameter-to-thickness ratio suffer a slightly larger deterioration in their cyclic response.

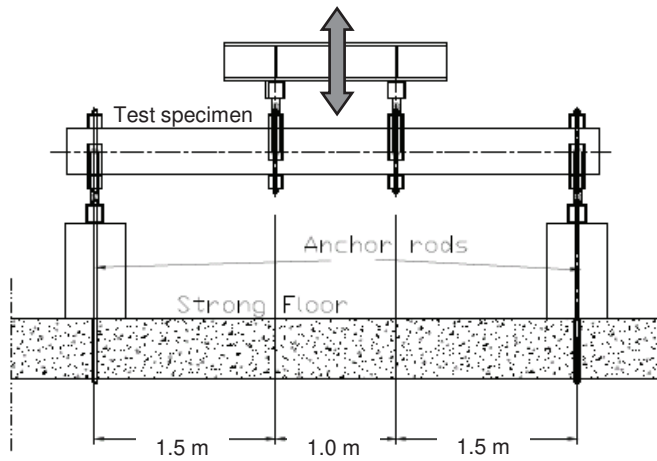
Future studies on the subject may incorporate non-linear accumulated damage models to assess accuracy with respect of relatively simpler linear models in predicting the time-dependent response.

REFERENCES

1. Shao, Yutian, and Mirmiran, Amir (2004) "Nonlinear Cyclic Response of Laminated Glass FRP Tubes Filled with Concrete," *Composite Structures*, 65(1): 91-101.
2. Ahmad, I. (2004) "Shear Response and Bending Fatigue Behaviour of Concrete-Filled Fibre Reinforced Polymer Tube," Ph.D. Thesis, North Carolina State University, Raleigh, NC.
3. Helmi, K., Fam, A., and Mufti, A. (2006), "*Behavior of Concrete Filled FRP Tubes under Fully Reversed Cyclic Bending*", *Arabian Journal of Science and Engineering*, 31(1C): 215 – 228.
4. Helmi, Karim (2006) "*The Effects of Driving Forces and Reversed Bending Fatigue of Concrete-Filled FRP Circular Tubes for Piles and Other Applications*," PhD dissertation, University of Manitoba, Winnipeg, Manitoba, Canada.
5. Helmi, K., Fam, A., and Mufti, A., (2005) "Field Installation, Splicing and Flexural Testing of Hybrid FRP/Concrete Pile" American Concrete Institute Special Publication ACI-SP 230, 7th International Symposium on Fiber Reinforced Polymer (FRP) Reinforcement for Concrete Structures, Kansas City, MO, USA.
6. Helmi, K., Fam, A., and Mufti, A., (2007) "*Static Testing and Fatigue Life Assessment of Structural GFRP Tubes Based on Coupon Tests*," Accepted for publication in the *Journal of Composites for Construction*, ASCE.
7. Deskovic, Nikola (1993) "Innovative Design of FRP Composite Members Combined with Concrete," Ph.D. thesis, Massachusetts Institute of Technology, Cambridge, Massachusetts, USA.
8. Ogin, S., Smith, P., and Beaumont, P. (1985) "Matrix Cracking and Stiffness Reduction During the Fatigue of (0/90)s GFRP Laminate," *Composites Science and Technology*, 22: 23-31.
9. Findley, W. (1960) "Mechanism and Mechanics of Creep of Plastics," *SPE Journal*, 57-65.
10. Holmen, J. (1982) "Fatigue of Concrete by Constant and Variable Amplitude Loading," *Fatigue of Concrete Structures*, ACI SP-75, Detroit, MI, 71-110.
11. Fam, Amir (2000) "Concrete filled Fiber Reinforced Polymer Tubes for Axial and Flexural Structural Members," PhD dissertation, University of Manitoba, Winnipeg, Manitoba, Canada.
12. Fam, A.Z., and Rizkalla, S.H. (2001) "Confinement Model for Axially Loaded Concrete Confined by Circular Fiber-Reinforced Polymer Tubes", *ACI Structural Journal*, 98(4): 451-461.
13. El-Tawil, S., Ogunc, C., Okiel, A., and Shahawy, M. (2002) "Static and Fatigue Analyses of RC Beams Strengthened with CFRP Laminates," *Journal of Composites for Construction*, ASCE, V. 5(4): 258-267.
14. Epaarachchi J.A., and Clausen P., "An Empirical Model for Fatigue Behaviour Prediction of Glass Fibre-Reinforced Plastic Composites for Various Stress Ratios and Test Frequencies", *Composites: Part A*, 34: 313-326.
15. Gamstedt, E., and Sjogren, B., (1999) "Micromechanisms in Tension-Compression Fatigue of Composite Laminates Containing Transverse Plies," *Composites Science & Technology*, 59:167-178.

Table 1 Summary of full-scale fatigue CFFT beam test program

Specimen ID	Source pile	M_{max}/M_{ult}	Frequency Hz	Testing machine capacity	Condition of termination
BFC3	C3	0.60	0.05	5000 kN	To failure (2,365) Cycles
BFP1U	P1	0.45	0.05	5000 kN	To failure (28,619) cycles
BFC1	C1	0.25	0.10	5000 kN	676532 cycles
		0.25	0.07	5000 kN	417782 cycles
		0.25	0.09	1000 kN	8556 cycles
		0.375	0.09	1000 kN	To failure (406,787) Cycles



(a) Schematic of test setup



(b) Support system

Fig. 1 Test setup



(a) Failure location



(b) Full depth crack

Fig. 2 Failure mode of specimen BFC3

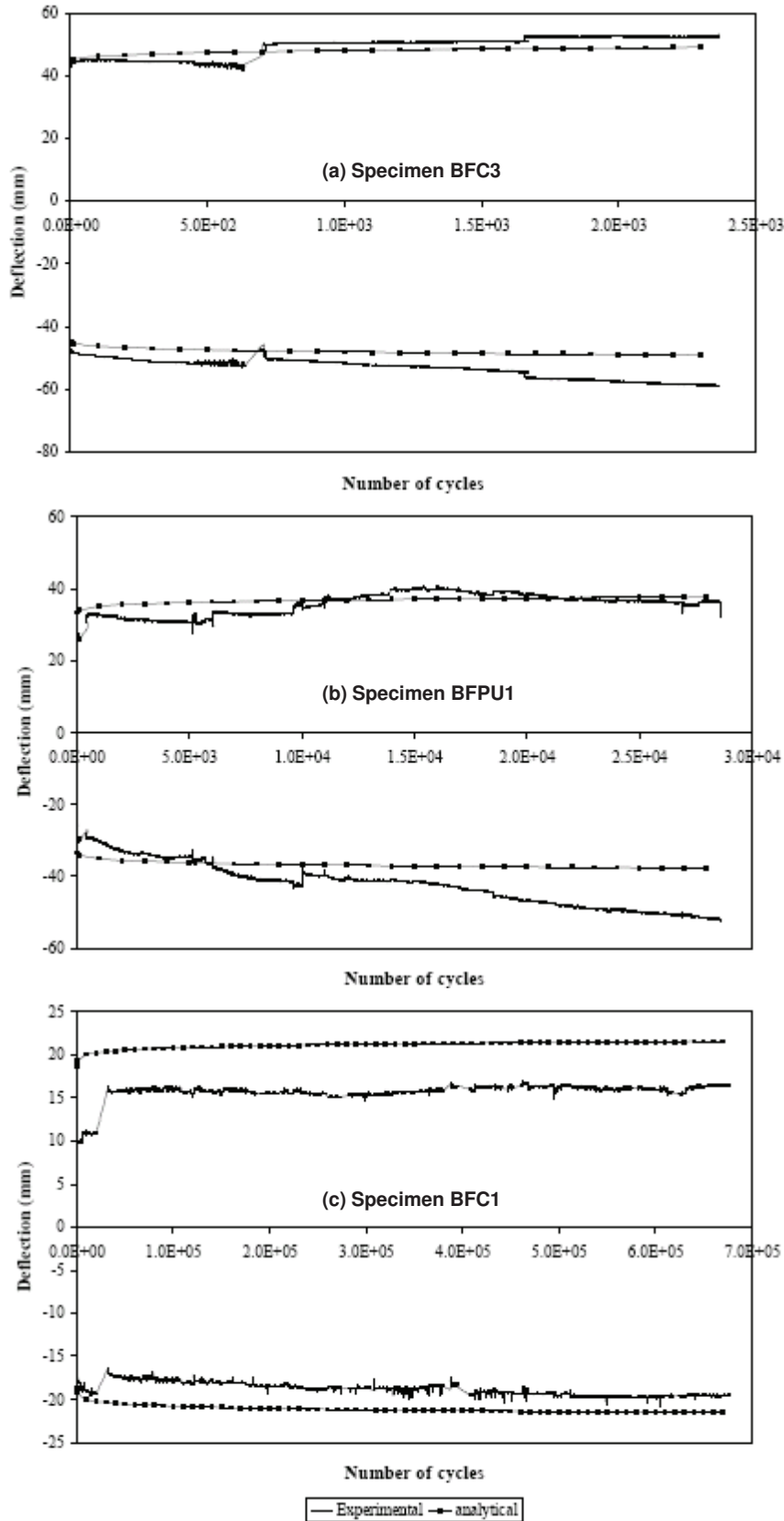


Fig. 3 Variation of midspan deflection with number of cycles (+ve deflection is downwards)

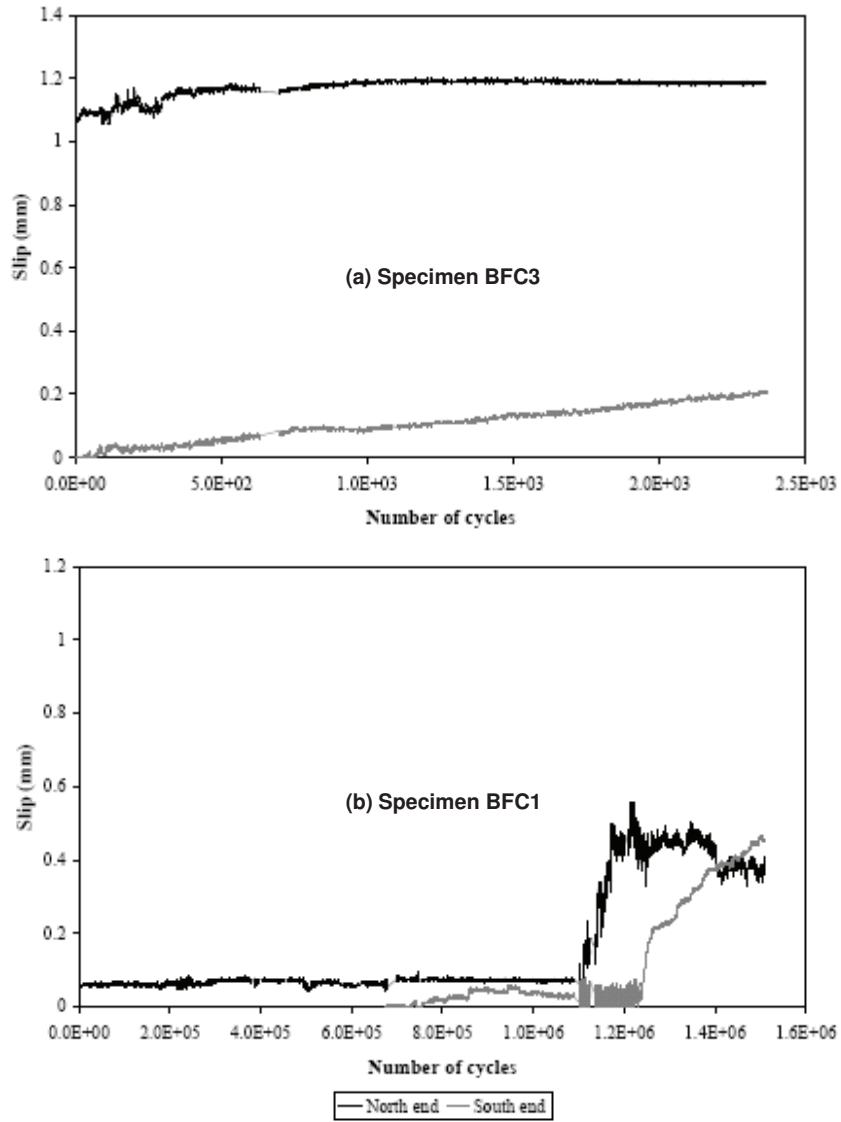


Fig. 4 Variation of end slip with number of cycles